

ON THE TECHNIQUE OF CORONAL MAGNETOGRAPHY THROUGH QUASI-TRANSVERSE PROPAGATION OF MICROWAVES

D.A. Bezrukov¹, B.I. Ryabov¹, V.M. Bogod², G.B. Gelfreikh³, V.P. Maksimov⁴, F. Drago⁵,
B.I. Lubyshev⁴, N.G. Peterova², T.P. Borisevich³

¹ *Ventspils International Radio Astronomy Center, Akademijas laukums 1, Riga LV-1050, Latvia*

² *Special Astrophysical Observatory, Nizhnij Arkhyz, 357147 Karachaevo- Cherkessia, Russia*

³ *Pulkovo Astronomical Observatory, Pulkovskoe shosse 65, 196140 Sankt-Petersburg, Russia*

⁴ *Institute of Solar-Terrestrial Physics, Lermontov str.126, 664033 Irkutsk, Russia*

⁵ *University of Florence, Department of Astronomy and Space Science, Largo Fermi 5, 50125 Florence, Italy*

Abstract. The technique of coronal magnetography is illustrated and analyzed on the samples of 4 solar active regions (ARs). The observational bases for the coronal magnetography are the radio maps of the Sun taken with the Siberian Solar Radio Telescope (SSRT) at the wavelength 5.2 cm both in I and V Stokes parameters. The magnetic field strength is found using the theory of wave mode coupling in the region of quasi-transverse (QT) propagation. The proper values are found to be in the range of 10 - 30 Gauss. The technique used is based on the fact that the circular polarization of a radio source is modified when the ray path crosses a region in the solar corona where the magnetic field is transverse to the line of sight. We have successfully applied this method to the whole period of transit on the solar disk of NOAA 9068, 9097, and NOAA 9339, while we have noticed some limitations of the coronal magnetography for the flare-productive active region NOAA 9415. The coronal magnetograms appear to be a series of 2D partial magnetograms, covering, on each day a part of the AR: the following part near the eastern limb and the leading one near the western limb. The technique has been verified to be reliable in the determination of coronal magnetic fields, but needs further improvements concerning the evaluation of their height, related to the heights of the QT-region.

Key words: Sun: radio emission, corona, magnetic fields.

1. INTRODUCTION

The coronal magnetic field measurements in a solar active region are of great interest for the studies of solar flares. Microwave observations are supposed to be the most direct way to provide the intensities of strongly localized coronal magnetic fields. However, the technique of the measurements needs a further improvement to be compatible with the forthcoming radio telescopes, such as the Frequency Agile Solar Radiotelescope (Gary, 2002).

In this paper we focus our attention to the variation of circular polarization in the site where the coronal magnetic field is perpendicular to the line of sight. The theory of the quasi-transverse (QT) propagation (Cohen, 1960; Zheleznyakov, 1970) predicts that the sign of circular polarization reverses if microwaves ray path crosses, almost perpendicularly, strong enough magnetic fields. The polarization is only slightly modified in case of weak coronal fields. It has been pointed out by Lee et al. (1998) that a moderate field in coronal QT-region appears as a zero circular polarization line (depolarization line, DL).

Figure 1 shows the variations of the QT-surface (where propagation angle α must be equal to 90°) with the longitudinal displacement of the AR. One can imagine a 3D quasi - transverse region (QTR), where the effect of QT-propagation is significant and the propagation angle is almost equal to 90° (Kravtsov and Naida, 1976; Segre and Zanza, 2001), extended to the distance

$\sim 10^8 - 10^9$ cm on both sides of the QT-surface. The thickness of the QTR along the ray path ($\sim 10^9$ cm) is less than its characteristic size within an AR ($\sim 10^{10}$ cm).

To illustrate the effect of the QTR, let us assume that the original circular polarization of a microwave source is uniform (Fig. 1). In this case the observed polarization can supply the strength of the magnetic fields in the QT-surface (in projection to image plane). In practice, the reduction to a uniformly polarized source (normalization procedure) is obtained by dividing each point of the QTR-affected polarization map by the not-QTR-affected map. The only problem is the availability of a radio image without any obvious QT-effects in circular polarization.

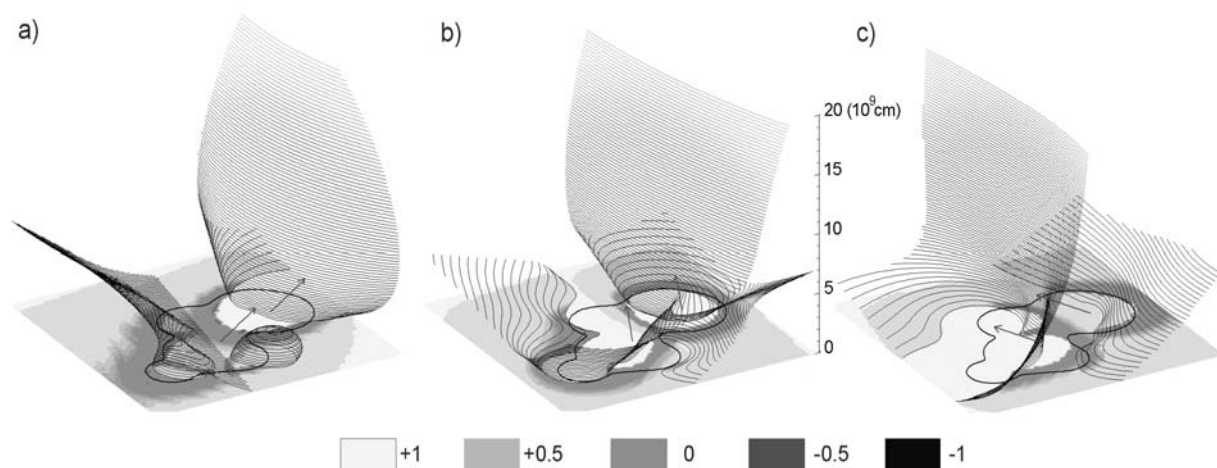


Fig. 1. The QT-surfaces presented as the loci where the rays (arrows) cross the coronal magnetic vectors at the right angle. The coronal field of AR 9068 at the longitudinal displacements: (a) $\theta = -48^\circ$, (b) $\theta = -6^\circ$, and (c) $\theta = +42^\circ$ from the central solar meridian is simulated by the superposition of 5 vertical dipoles. Grayscale images show the modification of circular polarization in the QTR in case that the original 5.2 cm radiation is uniformly polarized, $\rho = +1$, (the stronger the transformation is, the darker the area becomes).

The following characteristics, observed by Peterova, Akhmedov (1974); Maksimov, Bakunina (1991) and simulated by Ryabov (1981) are assumed to be a consequence of the QT-propagation of microwave radiation in a bipolar AR:

- The first region which inverts the sign of circular polarization in an AR is the sunspot-associated microwave source nearest to the solar limb;
- The depolarization line, $\rho = 0$, moves toward the western solar limb in the plane of view.

The pioneering work on 2D coronal magnetography of Ryabov et al. (1999) has pointed out some problems of the used technique:

- to determine the application areas and limitations of the technique;
- to make certain which method of estimating the heights of coronal magnetographic measurements in the QTR is the most accurate one;
- to outline the characteristic features of coronal magnetograms in terms of the geometry of an AR magnetosphere.

It seems appropriate to extend the coronal magnetography to a variety of ARs in order to solve the above mentioned problems and improve the technique. In Section 2 we present some ARs interesting for the coronal magnetography. A brief description of the coronal magnetography technique of the ARs undergoing to the QT-propagation effects will be given in Section 3. The application of this technique to the SSRT radio maps follows in Section 4. The problems associated with the QTR height evaluation are discussed in Section 5. Summary and conclusions are presented in Section 6.

2. RADIO MAPS

The Siberian Solar Radio Telescope (SSRT; see Grechnev et al., 2003) is daily used to take a radio map of the Sun in Stokes I and V at the wavelength 5.2 cm with an angular resolution $20''$. Four active regions, NOAA 9068, 9097, 9339, and 9415, are sampled to show the coronal magnetography procedure (Appendix 8). The four ARs have some common features:

- At least 1 inversion of the circular polarization sign is detected in each solar hemisphere during the AR transit;
- A magnetic axis of the associated sunspot group is directed predominantly in the east – west direction.

All active regions, except AR 9415, are associated with a stable sunspot group. The SSRT observations cover the whole period of transit of the ARs from the eastern to the western limb (Appendix 7). We have preferred ARs undergoing to polarization inversions in each solar hemisphere, since it supplies at least two sequences of coronal magnetograms. The east-west direction of the magnetic axis in the sunspot group makes it possible to attribute the polarization inversion to the effect of the QT-propagation of microwaves on the basis of a straightforward geometry. The wave path of the radiation coming from the limbward sunspot-associated source crosses perpendicularly the field lines connecting the sunspots of opposite magnetic polarity.

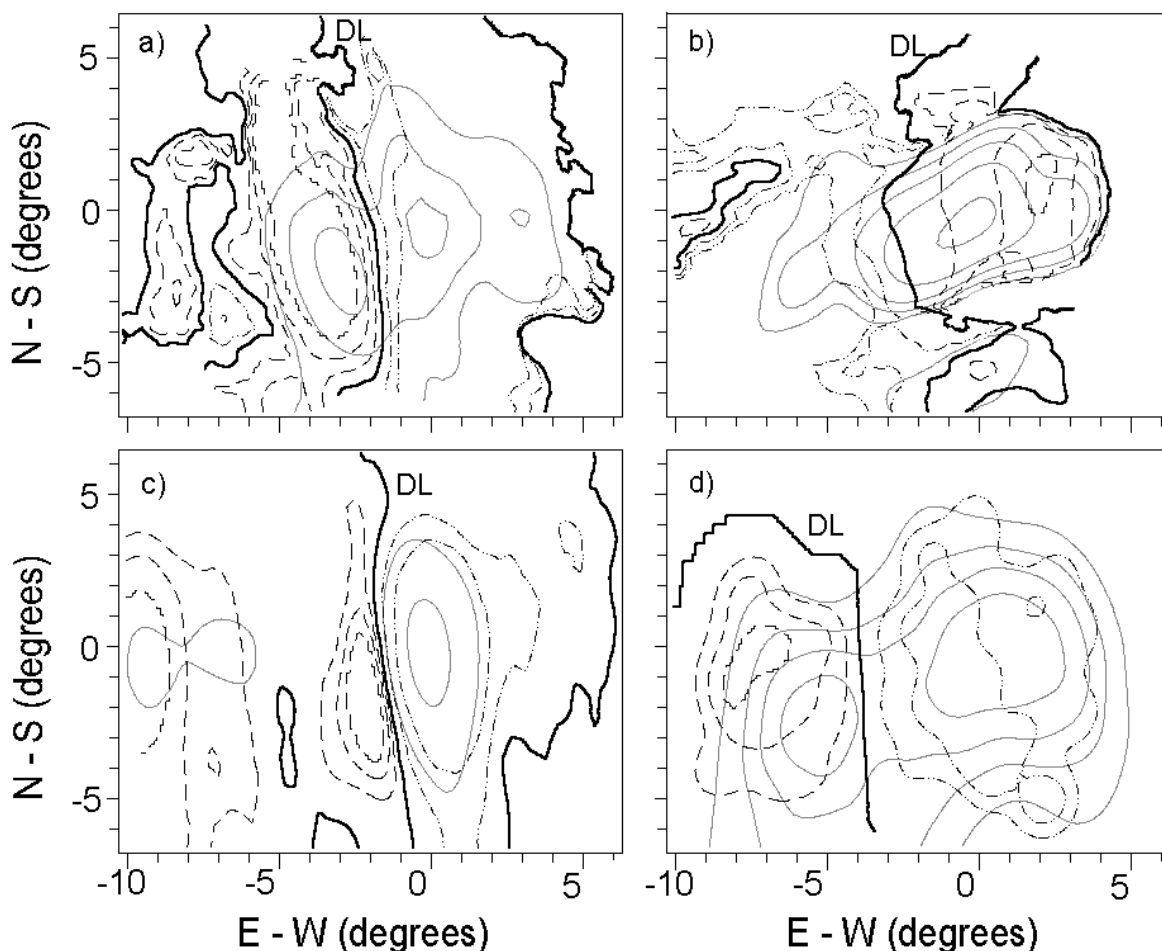


Fig. 2. SSRT radio maps of 4 solar active regions. The maps are taken on (a) 2000, July 6, 0:00 UT (NOAA 9068), (b) 2000, July 24, 0:00 UT (NOAA 9097), (c) 2001, February 9, 0:00 UT (NOAA 9339), and (d) 2001, April 9, 0:00 UT (NOAA 9415). The dashed (dash dot) contours represent degree of right (left) circular polarization at $[\pm 0.1, \pm 0.2, \pm 0.3]$ levels. The thick solid line represents a zero polarization line (DL). The solid contours correspond to the total radio intensity at $[1, 2, 5, 10] \times 10^5$ K. The maps are given in rectangular heliographic coordinates, with the origin located on the peak brightness in the total intensity. In Figs 2 – 8, the heliographic north is up, east is left.

The radio maps of circular polarization of bipolar ARs, taken near the center of the solar disk, denoted by ρ_0 ($\rho_0 = V_0/I_0$), are supposed to be free from the QT effects. Indeed, the comparison of the ρ_0 map (Fig.2a) with the photospheric magnetogram (Fig.3) clearly shows that the sign of the microwave polarization is consistent with the underlying magnetic polarity (assuming a prevalence of the extraordinary mode in the radio emission) almost everywhere over the microwave source. In Section 4 we will divide each point of the maps of circular polarization ρ by the corresponding point in the ρ_0 map. This procedure allows one to achieve a separation between the radiation and propagation effects in the observed polarization maps.

The bipolar character of the microwave source is evident, in ARs 9068 and 9415, also in the total intensity structure which represents two peaks on either sides of the zero polarization line (DL). As for the ARs 9097 and 9339, only one peak in total intensity is present, which appears displaced from the zero polarization line.

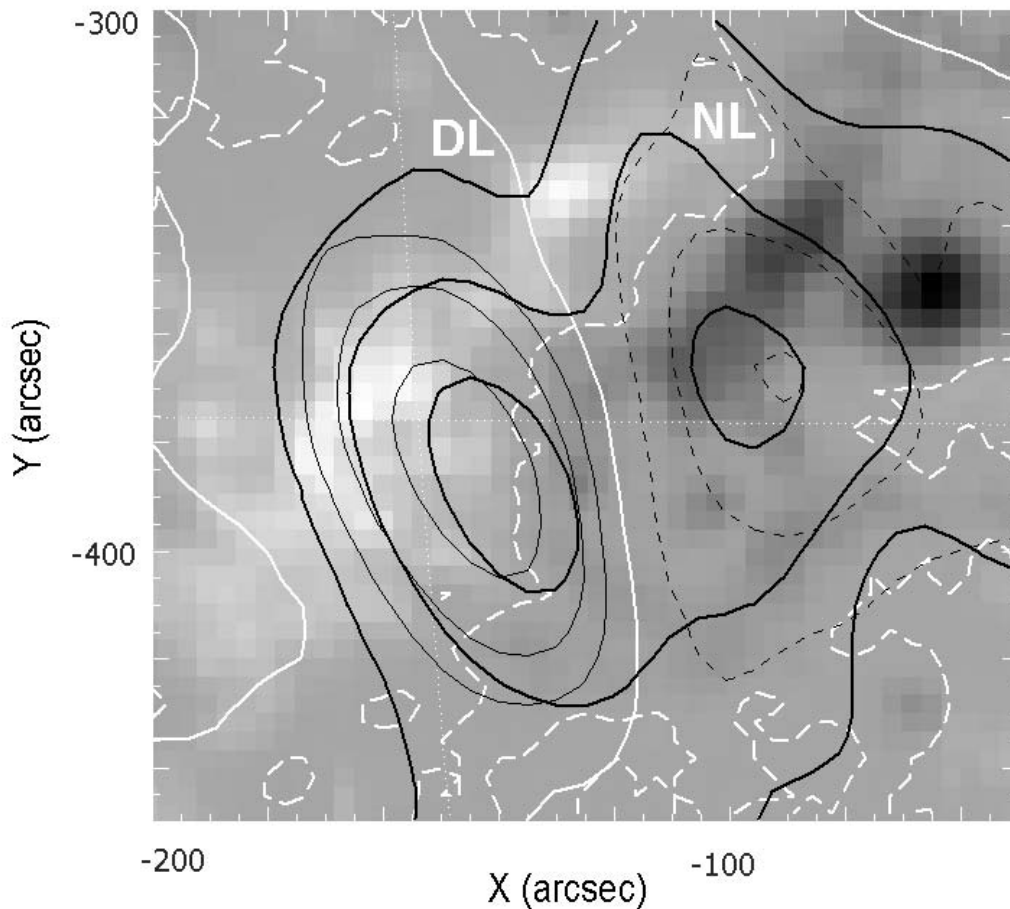


Fig. 3. Coaligned SSRT I and V maps of NOAA 9068 on July 6, 2000, taken between 5:53 – 6:36 UT, and a Kitt Peak National Observatory longitudinal magnetogram, taken within 15:29 – 16:24 UT. The magnetic neutral line (white dashed line) is marked NL. The line of zero circular polarization at 5.2 cm (white solid line) is marked DL.

For the active regions near the solar limb, the most limbward part of the microwave source has reversed the sign of its circular polarization. The zero polarization line, that is, the depolarization line (DL), is moving towards the western limb. Both these effects are in agreement with the results of QT-propagation at microwaves given by Bandiera (1982).

3. PROCEDURE

3.1. Relation between intrinsic and observable quantities

Let a sunspot-associated microwave source emit radiation with the circular polarization ρ_0 . If the radiation crosses a QT-region, the sign and the degree ρ of the resulting circular polarization depend on the following quantities present in the QTR: first of all the magnetic field strength B , then the electron density N and the scale of the magnetic field divergence L_α . If these two latter quantities are known, it is possible to infer the coronal magnetic fields from the observed ρ (Zheleznyakov and Zlotnik, 1964):

$$\rho = \rho_0 [2 \exp(-2 \delta_0) - 1]. \quad (1)$$

The coupling parameter reads (Zheleznyakov and Zlotnik, 1964):

$$2\delta_0 \approx 1.15 \times 10^{-25} B^3 N L_\alpha \lambda^4, \quad (2)$$

where λ is observing wavelength. Substituting (2) into (1) we may derive B , assuming $N L_\alpha = 10^{18} \text{ cm}^{-2}$ (Ryabov et al., 1999):

$$B \approx -2.05 \times 10^2 \lambda^{-4/3} \ln^{1/3} \left(\frac{\rho}{2\rho_0} + 0.5 \right). \quad (3)$$

The magnetic field divergence $L_\alpha = \alpha \left| \frac{d\alpha}{d\mathbf{l}} \right|^{-1}$ varies as the reciprocal of the gradient of propagation angle α (the angle between the propagation direction \mathbf{l} and the local magnetic field \mathbf{B}) in QTR.

For the wavelength $\lambda = 5.2 \text{ cm}$ and putting $P = \rho/\rho_0$, the coronal magnetic field B (in Gauss) reads:

$$B \approx -22.8 \ln^{1/3} (0.5 P + 0.5). \quad (4)$$

From the above equation a 2D coronal magnetogram can be evaluated. The normalized degree of circular polarization P is sensitive only to the QT-propagation and not to the emission mechanism. A coronal magnetogram supplies the magnetic field strength in the QT-region, which is well above the height of the microwave emission.

3.2. Normalization procedure

When the source is near the solar disk center, the QTR is crossed higher up in the corona, where the magnetic field B is weak and the resulting polarization ρ is the same as it was before crossing the QTR, that is, ρ_0 . As the source moves towards the western solar limb the QTR is crossed at lower levels in the corona and the sign of the resulting circular polarization is reversed. The technique is most sensitive for $\rho \approx 0$, that is $P \approx 0$, at which corresponds a magnetic field strength $B \approx 20 \text{ G}$.

In order to get the largest number of informations from equation (4), Ryabov et al. (1999) have used the full range (-1, +1) of the normalized degree of circular polarization P . The

procedure starts with the selection of a radio map with the degree of circular polarization, $\rho_0 = V_0/I_0$, suitable for the normalization of a set of AR polarization maps with different values of ρ . A map is suitable if there is no evidence of polarization inversion. As an example, a radio source associated to a bipolar AR, without any polarization inversion, looks like a bipolar microwave source.

The next step is to shift all maps with $P(= \rho/\rho_0) < 1$ to the position of the normalization map, which is usually found to be near the central meridian. The shift is made by imposing that the position of the peak of the total intensity map, I , coincides with the peak I_0 of the normalization map.

Finally, the normalized P maps are converted into coronal magnetograms using the equation (4). The borders of the coronal magnetograms are derived from the reasonable limitation of $|P| < 1 - \sigma = 0.95$. The value of σ determines the relative accuracy of the ρ maps. In case of SSRT observations, $\sigma = 0.05$.

The following assumptions must be satisfied in order to perform the coronal magnetography:

- (a) The normalization ρ_0 map is free from the effects of QT – propagation.
- (b) In principle the microwave source should not evolve during the period in which the coronal magnetograms are derived. However in all cases we have noticed some changes in a portion of it and therefore the normalization problem persists.
- (c) The QT - effect is not complex, namely it is due to only one crossing of the QTR.
- (d) The approximation of $NL_\alpha = 10^{18} \text{ cm}^{-2}$ is valid throughout the QTR used for the coronal magnetography derivation.
- (e) All radio maps used are precisely calibrated.

3.3. The accuracy of normalization procedure

The accuracy of the normalization procedure can be checked by means of spectral polarization observations made by the radio telescope RATAN-600. Since the points where the observed polarization is $V = 0$ must coincide with the points where $P = 0$ independently of the normalization procedure, the position of $V = 0$ line is the same as the position of the $P = 0$ line. Hence, the $V = 0$ points in the RATAN-600 V scan can be compared with the corresponding $P = 0$ points in the normalized P map of SSRT at the same wavelength. Moreover, if the normalization procedure is precise, $V = 0$ points in V scans, at a wavelength different from 5.2 cm, but close enough to it, should coincide with the corresponding $P = \text{constant}$ point in the P map at 5.2 cm (or with the corresponding $B = \text{constant}$ point in the coronal magnetogram). The correspondence is given by Eqs (1) - (4), provided NL_α is constant. As an example, the $V = 0$ point at 4.93 cm, supplies, through Eq. (3), a magnetic field $B \approx 21.6$ G. The position of the point $V = 0$ in 1D radio scan taken with the RATAN-600 at 4.93 cm should therefore coincide with the 21.6 G line position in the coronal magnetogram measured with the SSRT ($P \approx -0.145$ at 5.2 cm; cf. Fig. 8).

4. CORONAL MAGNETOGRAMS

In Figures 4 - 7 some coronal magnetograms of the four analysed ARs are presented. The 2D magnetograms are calculated according to the technique described above. The minimum value of the normalized degree of circular polarization we are dealing with is -0.95, which, according to Eq.4 corresponds to the strongest magnetic field detectable at 5.2 cm in the QTR: $B = 35$ G. The weakest coronal field detectable with the SSRT is $B = 7$ G, which corresponds to $P = +0.95$. The

photospheric neutral line (NL in Fig. 4), $B_l = 0$, is the lowest border of the QTR located at the photospheric level.

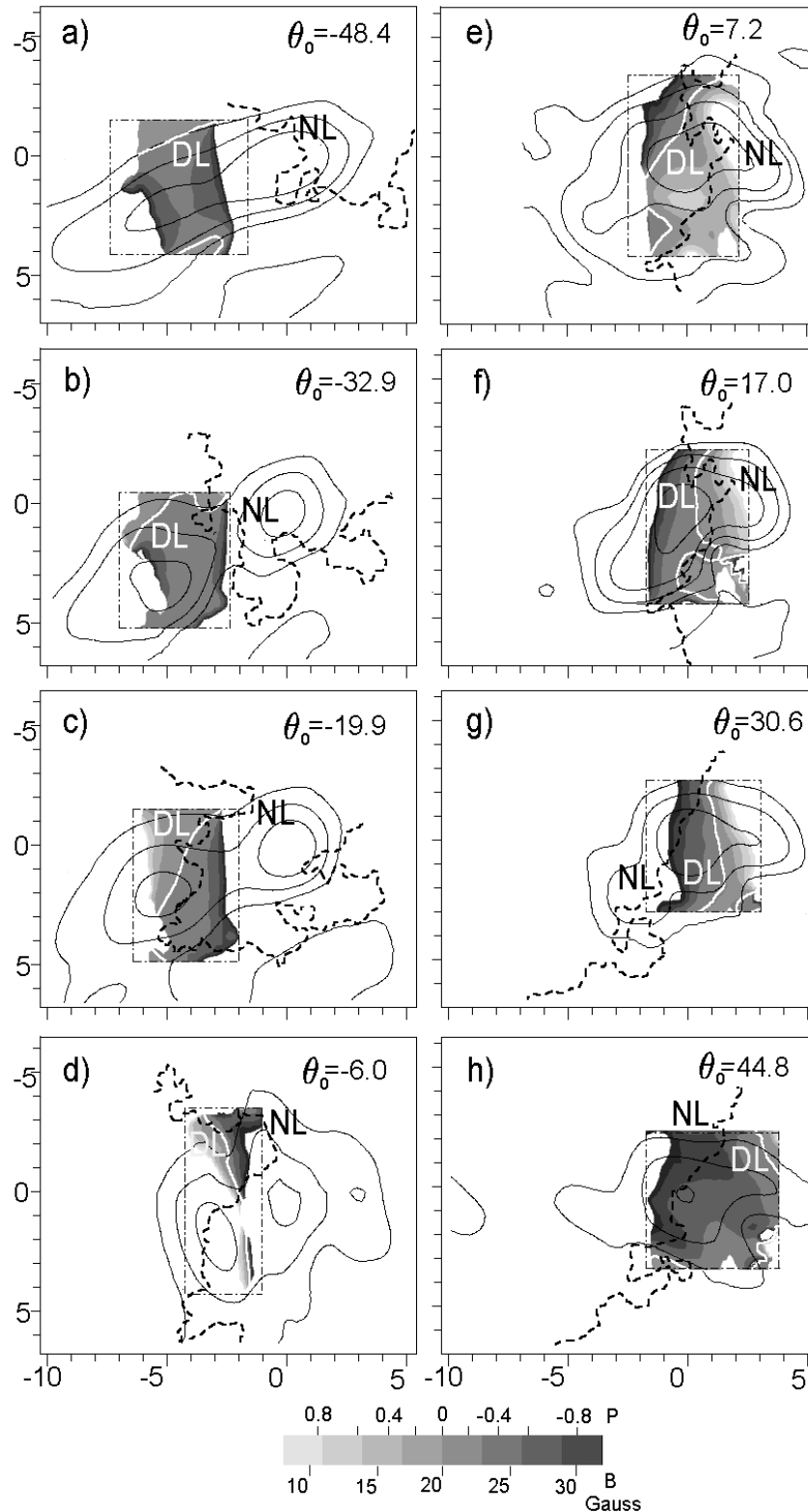


Fig. 4. A series of daily coronal magnetograms of the NOAA 9068 at several longitudinal displacements θ_0 from the central solar meridian on (a) July 3, (b) July 4, (c) July 5, (d) July 6, (e) July 7, (f) July 8, (g) July 9, and (h) July 10, 2000. The solid contours correspond to the total radio intensity at $[1, 2, 5, 10] \times 10^5$ K observed with the SSRT at the wavelength of 5.2 cm., while the grey scale supplies both the normalized circular polarization P at the same wavelength and the coronal magnetic field strength B (Gauss) in the QT-surface when projected to the image plane. The box with dash - dot line indicates the

magnetogram area clipped outside the microwave source. The maps are given in rectangular heliographic coordinates, with the origin located on the peak brightness in the total intensity. Ticks mark 1° intervals.

The photospheric magnetic neutral line (NL, black dashed line) is projected from Kitt Peak National Observatory magnetograms. Note the westward displacements of the zero circular polarization line (DL, white solid line) with time (through the panels (a) – (h)).

An obtainable coronal magnetogram can be defined as the distribution of magnetic field strength in the QT-surface, projected on the image plane. We will focus our attention on some particular features to prove the magnetographic nature of the normalized radio maps. Our discussion will also focus on the QT-surface itself since it represents a large-scale outline of the active region magnetosphere, if the line of sight direction is taken into consideration. The coronal magnetography is applicable to rather limited portion of the AR on each day, as indicated by Figures 4 - 7.

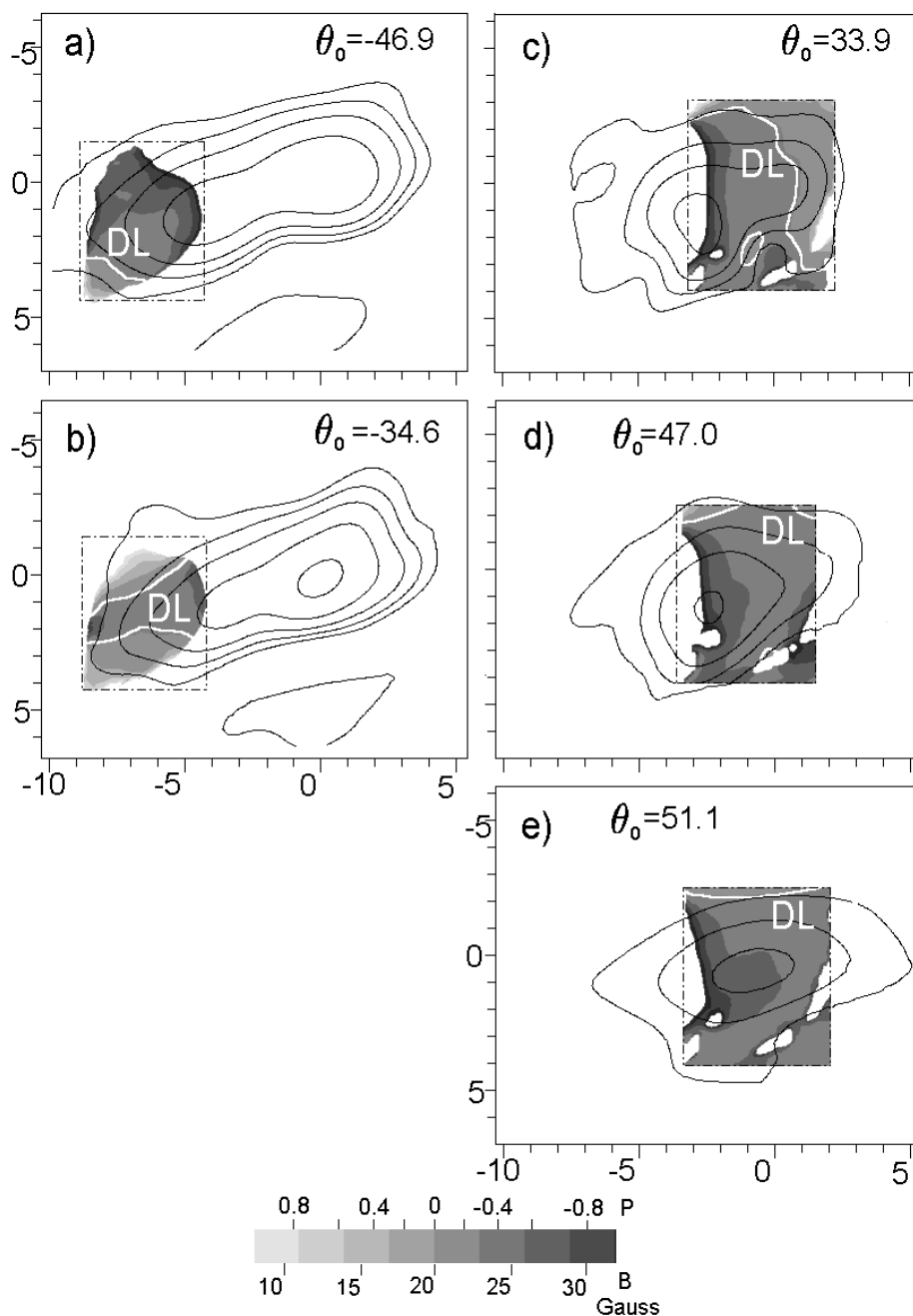


Fig. 5. A similar representation as in Fig.4 for NOAA 9097 on (a) July 21, (b) July 22, (c) July 27, (d) July 28, and (e) July 29, 2000.

The geometry of the QT-surface is quite obvious in case of a bipolar AR with the magnetic axis parallel to the solar equator (Ryabov, 1981). If no new magnetic fluxes appear in an AR, the shape of the QT-surface is modified only by the solar rotation. The geometrical characteristics are the following: (Ia) On a large scale the QT-surface appears as an inclined conical surface surrounding one sunspot. The QT-surface is located in the central part of a bipolar active region or, more precisely, above the photospheric neutral line. (IIa) The photospheric neutral line is always the lower border of the QT-surface. (IIIa) The QT-surface is slightly inclined toward the line of sight, as shown in Fig. 1.

The representative characteristics of the coronal magnetograms arise from the QT-surface characteristics and the general tendency of the coronal magnetic fields to decrease with height, becoming more regular. Let us use the derived coronal magnetograms to illustrate two characteristics: (Ib) The depolarization line, as well as any $P = \text{constant}$ line in the image plane, moves toward the western solar limb during the AR transit on the solar disk (Figs 4, 5, 7). (IIb) The coronal fields gradient is directed east – west in the image plane for the magnetograms in the eastern hemisphere (Figs 4c and 5a - 5b) and west - east for those in the western hemisphere (Figs 4e - 4h and 5c – 5e).

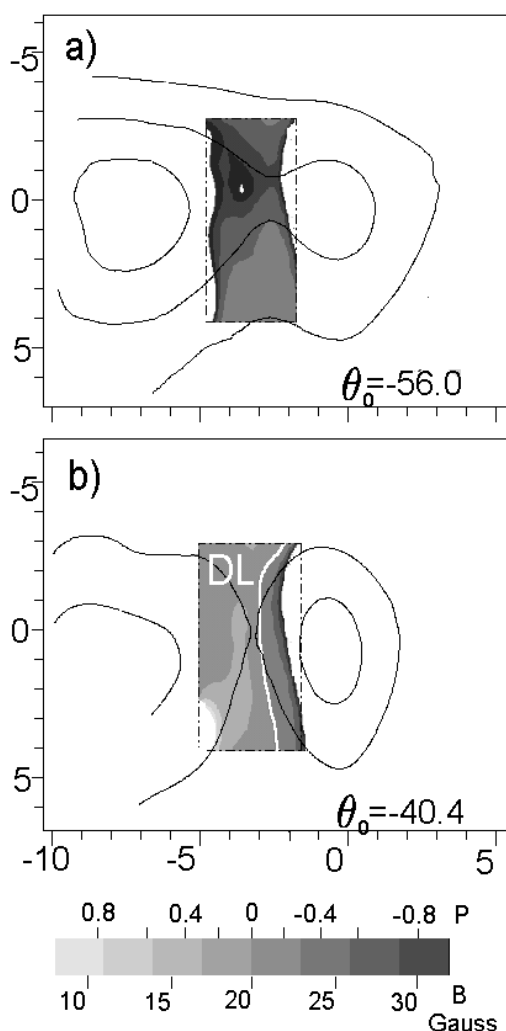


Fig. 6. A similar representation as in Fig. 4 for NOAA 9339 on (a) February 6, (b) February 7.

It must be pointed out that there are some unclear features present in the derived coronal magnetograms:

- As the AR approaches the solar limb, an inversion of the coronal magnetic field gradient may appear in the limbward part of these magnetograms (Figs 4a, 4b, and 5d). We

suppose that these features originate from a polarization inversion in the limbward parts of the normalizing map (relate Fig. 2a to Fig. 4a).

- There are gaps in some magnetograms which seem to coincide with the maximum radio brightness (or with the minimum brightness in Fig. 4f) or with the DL in the normalizing ρ_0 map (cf. Fig. 2b and Figs 5c - 5e). We find that the latter features are due to the division by zero.

From what previously mentioned, the following cautions in the coronal magnetography technique must be taken into account:

- If regions with inverted initial polarization do appear in the normalizing map ρ_0 , the corresponding regions of coronal magnetograms must be eliminated.
- The most reliable magnetography is expected within the dominant bipolar microwave sources around the central DL in an AR.
- Nearby DLs and microwave sources associated with parasitic magnetic polarities additional analysis are needed.

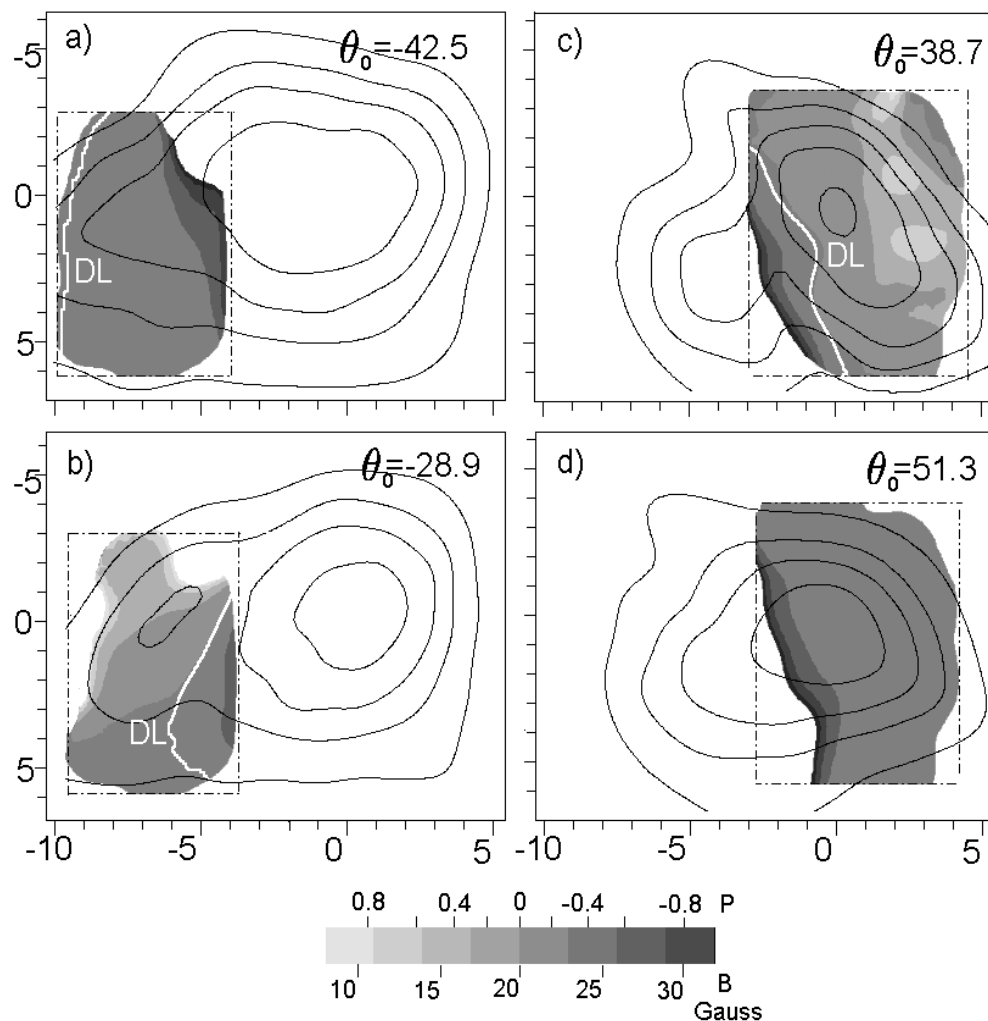


Fig. 7. A similar representation as in Fig. 4 for NOAA 9415 on (a) April 6, (b) April 7, (c) April 12, and (d) April 13, 2001.

The coronal magnetography accuracy is limited by the accuracy of the measurement of the circular polarization degree, which is assumed $\sigma = 0.05$ for the SSRT measurements. The angular resolution of the coronal magnetograms is the same as that of the radiotelescope which supplies the radio maps. ($20''$ in the case of the SSRT according to Grechnev et al., 2003.) The range of measurable coronal fields can be determined by Eq. (3) for a given wavelength λ and

for $|P| < 1 - \sigma$, turns out to be 7 – 35 G for SSRT observations. We may determine the accuracy of coronal magnetograms derived from radio measurements as well as and the accuracy of the normalization procedure, by using 1D spectral polarization observations obtained with the radiotelescope RATAN-600.

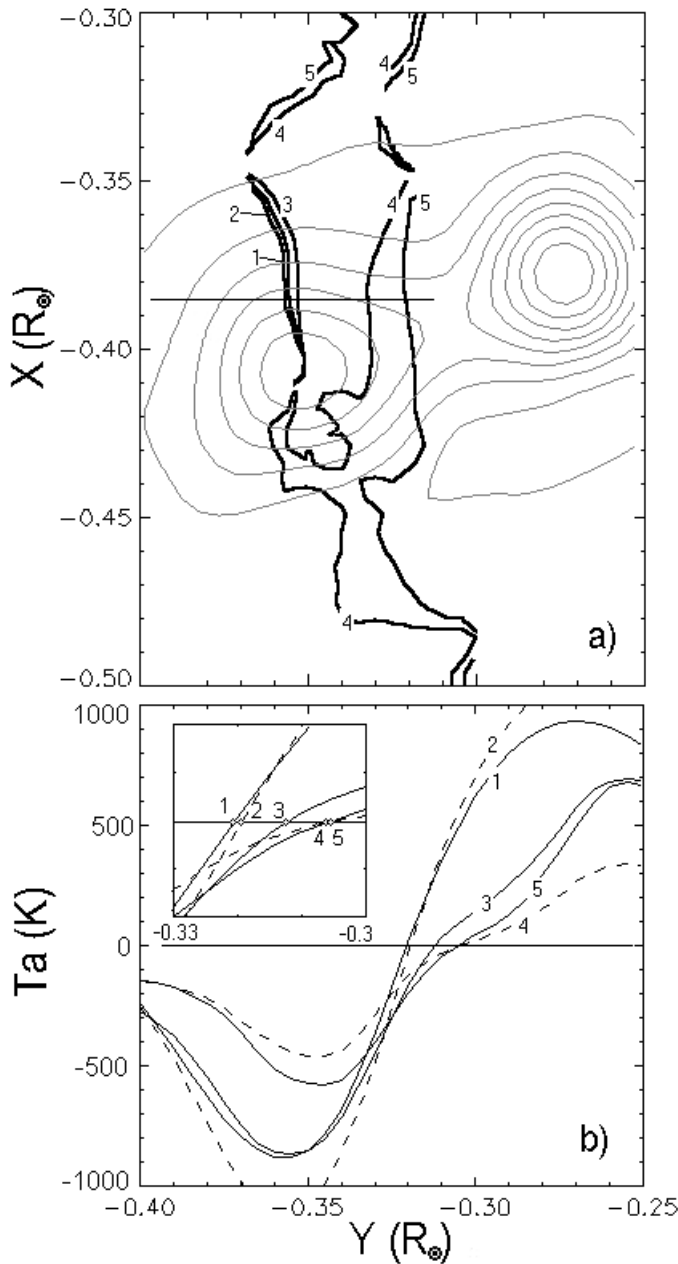


Fig. 8. NOAA 9068 on July 5, 2000. Comparison of the SSRT coronal magnetogram with the position a set of RATAN-600 V scans.

- (a) Radio I map (thin lines) taken at the SSRT wavelength of 5.2 cm with the magnetic field contours determined from the polarization inversion (thick lines):
- 1 - 13.5 G,
 - 2 - 14.9 G,
 - 3 - 16.2 G,
 - 4 - 21.6 G, and
 - 5 - 23.6 G.
- (b) Radio V scans taken by the RATAN-600 at the following wavelengths:
- 1 - 7.02 cm,
 - 2 - 6.52 cm,
 - 3 - 6.06 cm,
 - 4 - 4.93 cm, and
 - 5 - 4.61 cm.

Figure 8 shows the comparison of a coronal magnetogram, derived from a SSRT normalized P map, obtained with the SSRT, with the east - west scans of the circular polarization, obtained from RATAN-600. According to SSRT coronal magnetogram of July 5, 2000 (NOAA 9068), the magnetic field gradient, along the direction of the RATAN-600 scanning, is equal to $5 \times 10^{-9} \text{ G cm}^{-1}$. The zero points on RATAN-600 V scans, resulted from the QTR depolarization at a set of wavelengths, provide a gradient equals to $8 \times 10^{-9} \text{ G cm}^{-1}$. The latter estimate is made by means of Eq. (3): taking $\rho = 0$ (zero point) at the wavelength λ of 7.02 cm, 6.52 cm, 6.06 cm, 4.93 cm, and 4.61 cm, one gets B equal to 13.5 G, 14.8 G, 16.4 G, 21.6 G, 23.6 G correspondingly. One can conclude that the measured magnetogram is less compact by a factor 0.6 than that expected by the zero polarization points observed by RATAN-600. However, some improvements are

required in the comparison procedure used to match a coronal magnetogram with the V scans taken with the fan-beam antenna of RATAN-600.

Before the analysis of P-maps, we should better investigate the position of the microwave sources using model simulations of the AR magnetospheres. For instance, in the microwave source related to NOAA 9415, a double polarization inversion was present (Bogod et al., 2003) against the assumption (c) in Section 3.2. It is interesting to note that all P maps (Figs. 4 – 7) show the representative geometrical characteristics (Ib) – (IIb) of coronal magnetograms. Another problem can arise if a thermal microwave source is located at the top of a coronal loop. If the microwave radiation coming from this source crosses the QT-surface on the way to the observer, the radiation and propagation effects may be combined to form a modified depolarization line (Alissandrakis and Preka-Papadema, 1984; Alissandrakis et al., 1993). A more detailed analysis of four ARs under consideration will be published elsewhere.

5. HEIGHT EVALUATION

A magnetogram usually supplies, at best, the distribution of the magnetic field vectors measured on a surface of known shape and position. In case of coronal magnetograms derived from QT-propagation effects, we should know the coordinates of the inferred magnetic field, namely its heights and the angles between the field vector and a reference direction ('azimuth') which cannot be directly derived from microwave observations. Once the height and the azimuth of the field vectors are known, one can determine the height and shape of the QT-surface and reconstruct the 3D picture of the coronal magnetic fields. Strictly speaking, the coronal magnetography measurements refer to the coronal QT-region in projection to the image plane. In this Section we shall attempt to evaluate the height of the measured magnetic fields (namely the height of the QTR).

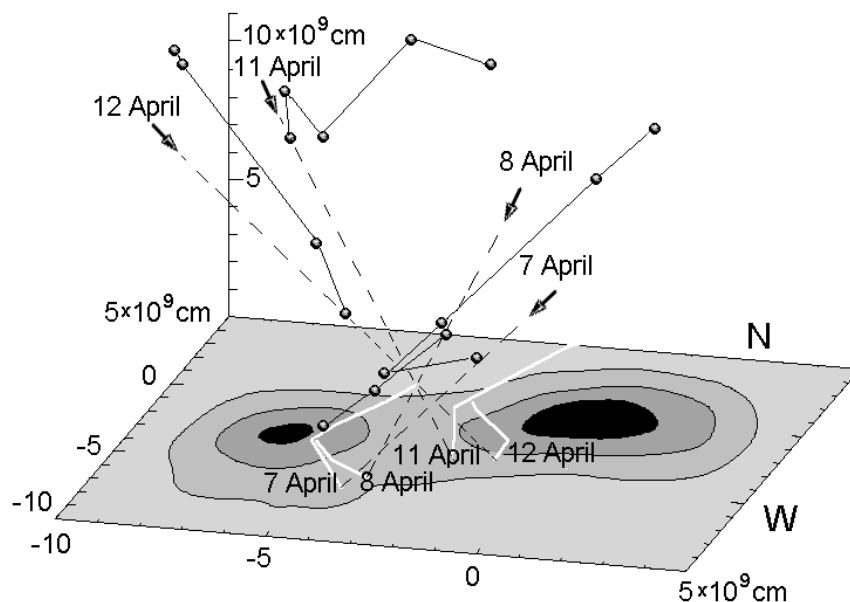


Fig. 9. QT-surface positions (open circles) determined for active region NOAA 9415 on April 7, 8, 11, and 12, 2001. Each position is found from the height at which the magnetic field vector with the strength $B = 21$ G is perpendicular to the direction of the wave propagation (arrow) on the way from the $P = -0.1$ line in the microwave source (white solid line) to the observer. Coronal height is evaluated from the apparent movement of the $P = -0.1$ line due to the solar rotation (Appendix 8).

The height of the QTR can be determined, using radio observation, either from the displacement of the depolarization line with respect to the photospheric neutral line (Kundu and

Alissandrakis, 1984; Alissandrakis, 1999), or from the averaged rate of inversion at 5.2 cm (Peterova, 1975; Gelfreikh et al., 1987). It can be also directly calculated using the extrapolation of the photospheric magnetic field at coronal levels (Alissandrakis et al., 1996; Lee et al., 1998; Ryabov et al., 2004). All methods of height evaluation are affected by a large uncertainty (up to about a factor of 2). In this paper we follow a new method for the QTR height evaluation (detailed in Appendix 8 and exemplified in Fig. 9). With this method we may drop the assumption of a not-evolving AR (assumption (b) in Section 3.2).

It is clear that the higher is a $B = \text{constant}$ line, the faster its projection moves in the plane of view. However this effect cannot be easily put in light for interferometric observations of faint microwave sources. Table I of Appendix 7 summarizes the results of the measurements of QTR height associated with the displacement of $B = 21$ G line (according to Eq. (4) $B = 21$ G corresponds to $P = -0.1$ line, which is taken to determine the displacement). We note a wide dispersion of the results ($0.062 \pm 0.035 R_{\odot}$ for AR 9068; $0.105 \pm 0.049 R_{\odot}$ for AR 9097; $0.085 \pm 0.021 R_{\odot}$ for AR 9415) with the mean height equal to 5.8×10^9 cm. Contrary to NOAA 9415, the QTR height values in AR 9068 and AR 9097 are larger in the eastern than in the western hemisphere, that is, above the following sunspots of the AR which has a lower magnetic flux. The parasitic magnetic polarities within the sunspots of AR 9415 are supposed to be the reason for the double polarization inversions and for the complicated displacements of the depolarization line at 5.2 cm (Bogod et al., 2003). In our opinion, the decreasing QTR height with the increasing displacement from the central solar meridian, noticed in AR 9097 is due to the compact configuration of the sunspot group. The reason is that the magnetic field strength decreases as the QTR moves from the center of the sunspot group with the displacement of the AR from the central meridian.

6. SUMMARY AND CONCLUSIONS

The technique of the 2D coronal radio magnetography, derived from the polarization inversion phenomenon which may take place where the wave propagation is quasi-transverse (QT) to the local magnetic field, has been outlined by Gelfreikh et al., 1987 and applied, later on, by Ryabov et al., 1999. In the later paper a coronal magnetogram was derived over a bright microwave source observed with the NoRH at 1.76 cm in total intensity and polarization. In this paper we present the coronal magnetograms of some solar active regions observed with the radio heliograph SSRT, at the wavelength 5.2 cm. The active regions were followed and the corresponding coronal magnetograms were derived both in the eastern and western solar hemisphere. The following conclusions can be drawn from the present work on coronal magnetography:

- I. SSRT observations of four active regions, NOAA 9068, 9097, 9339, and NOAA 9415, give evidence of the QT-propagation effects: the polarization inversion takes place in the limbward part of microwave source when the AR is displaced from the central solar meridian. The wavelength dependence of circular polarization is given by Eq. (1) (as proved by Bogod et al., 2003 for the case of AR 9415). It is found that the features of the measured coronal magnetograms are consistent with the geometry of QT-surface and with the general tendency of the coronal magnetic fields to decrease with height. In fact observations of the SSRT at the wavelength of 5.2 cm supply coronal fields of 6.7 – 35 G weaker than 28 – 150 G inferred from the 1.76 cm maps taken by the NoRH, with observational evidence for a lower level in the QTR for the modification of the 1.76 cm circular polarization than the level of the modification at 5.2 cm (Ryabov et al., 1999; Ryabov et al., 2004).
- II. We have pointed out that the depolarization line, $V = 0$, in the image plane does not depend on in the normalization procedure. Therefore, we have checked the accuracy of

the normalization procedure using multi-wavelength observations, around $\lambda = 5.2$ cm, performed with the RATAN-600 radiotelescope. This check is very important in the coronal magnetography technique since the radio map chosen for the normalization is taken 1 – 4 days apart from that used to produce a coronal magnetogram. Possible changes of the microwave source in this time interval can alter the resulting magnetogram.

- III. We have elaborated a new method for the determination of the height of the inferred magnetic fields in the coronal magnetograms. This is compared with existing semi-empirical methods: an inaccuracy of several tens percent is present in all methods. The knowledge of the position of the microwave source undergoing to polarization inversion/change in the QTR will improve the accuracy of the height determination.

The main conclusion of this work is that, using the coronal magnetography technique, we may derive measurements of coronal magnetic fields from radio observations. The inferred magnetic fields refer to the period during which the polarization inversion is observed and depend on observing wavelength. Coronal fields of 1 – 180 G can be measured over an area up to $\sim 50'' \times 100''$ (the size of the portion of a microwave AR affected by polarization inversion), if the AR is observed, in total intensity and polarization, during a period of 4 – 7 days in the wavelength range of 1 - 50 cm. This type of observations will be possible with a dedicated Solar Radiotelescope as the forthcoming Frequency - Agile Solar Radiotelescope (see the Web site http://www.ovsa.njit.edu/fasr/author_info.html).

ACKNOWLEDGMENTS. This work has been supported by the INTAS Open Call 2000 grants 00-0181 and 00-0543.

REFERENCES

- Alissandrakis, C.E. 1999, *Proc. of Nobeyama Symp.*, NRO Report **479**, 53.
 Alissandrakis, C.E., Borgioli, F., Chiuderi Drago, F., Hagyard, M., Shibasaki, K. 1996, *Solar Phys.*, **167**, 167.
 Alissandrakis, C.E., Nindos, A., Kundu, M.R.: 1993, *Solar Phys.*, **147**, 343.
 Alissandrakis, C.E. and Preka-Papadema, P. 1984, *Astron. Astrophys.*, **139**, 507.
 Bandiera, R. 1982, *Astrophys.J.*, **112**, 52.
 Bogod V.M., Gelfreikh G.B., Drago F.Ch., Maksimov V.P., Nindos A., Kaltman T.I., Ryabov B.I., Tokhchukova S.Kh. 2003, *ASTROPAGE*, paper: astro-ph/03009444, <http://lanl.arxiv.org/abs/astro-ph/?astro-ph%2F0309444>
 Brosius, J.W., Davila, J.M., Thomas, R.J., White, S.M. 1997, *Astrophys. J.*, **488**, 488.
 Cohen, M.H. 1960, *Astrophys. J.*, **131**, 664.
 Gary, D.E. 2002, *Journal of the Korean Astronomical Society*, **35**, 1.
 Gelfreikh, G.B., Peterova, N.G., Ryabov, B.I. 1987, *Solar Phys.*, **108**, 89.
 Grechnev, V.V., Lesovoi, S.V., Smolkov, G.Ya., Krissinel, B.B., Zandanov, V.G., Altyntsev, A.T., Kardapolova, N.N., Sergeev, R.Y., Uralov, A.M., Maksimov, V.P., Lubyshev, B.I., 2003, *Solar Physics*, **216**, 239.
 Kravtsov, Yu.A., Naida, O.N. 1976, *Soviet Phys. – JETP*, **44**, 122.
 Kundu, M.R. and Alissandrakis, C.E. 1984, *Solar Phys.*, **94**, 249.
 Lee, J., White, S.M., Kundu, M.R., Mikic, Z., McClymont, A.N. 1998, *Solar Phys.*, **180**, 193.
 Maksimov, V.P. and Bakunina, I.A. 1991, *Soviet Astron.*, **35**, 194.
 Peterova, N.G. 1975, *Soln. Dann. Bull.*, **3**, 96 (in Russian).
 Peterova, N.G., Akhmedov, Sh.B. 1974, *Soviet Astron.*, **17**, 768.
 Ryabov B. 1981, *Issledovanija Solnca i Krasnyh Zvezd*, **15**, 5 (in Russian).
 Ryabov, B.I., Pilyeva, N.A., Alissandrakis, C.E., Shibasaki, K., Bogod, V.M., Garaimov, V.I., Gelfreikh, G.B. 1999, *Solar Phys.*, **185**, 157.

- Ryabov B.I., Maksimov V.P., Lesovoi S.V., Shibasaki K., Nindos A., Pevtsov A.A. 2004, *Solar Physics*, (submitted).
- Segre, S.E., Zanza, V. 2001, *Astrophys. J.*, **554**, 408.
- Zheleznyakov, V.V. and Zlotnik, E.Ya. 1964, *Soviet Astron.*, **7**, 485 .
- Zheleznyakov, V.V. 1970, *Radio Emission of the Sun and Planets*, Oxford, Pergamon Press.

APPENDIX 7: CHARACTERISTICS OF SAMPLED ACTIVE REGIONS

Table I. Heliographic position, sense of circular polarization of the dominant microwave source, and QTR height of 21 G line determined from SSRT observations at 5.2 cm.

Active region Date of CMP	Characteristic	Time interval (in days) from the time of central meridian passage (CMP)								
		-4	-3	-2	-1	0	+1	+2	+3	+4
NOAA 9068 July 6, 2000	Latitude (deg)		-19.27	-18.96	-19.18	-19.89	-18.17	-17.24	-18.14	-18.01
	Longitude (deg)		-48.44	-32.93	-19.93	-6.02	7.22	17.07	30.55	
	Right/left sense of c. p.		L	L	L	R/L	R/L	R	R	R
	QTR height (R_{\odot})*		0.133	0.036	0.079	-	0.055	0.037	0.045	0.047
NOAA 9097 July 25, 2000	Latitude (deg)	6.03	5.03	6.55	5.75	5.44	6.13	6.86	7.03	7.66
	Longitude (deg)	-46.94	-34.6	-20.8	-7.19	8.09	21.1	33.98	47.02	59.1
	Right/left sense of c. p.	R	R	R	L/R	L/R	L/R	L	L	L
	QTR height (R_{\odot})*	0.059	0.082	0.178	-	-	-	0.131	0.073	
NOAA 9339 Feb. 10, 2001	Latitude (deg)	-10.21	-9.2	-10.16	-10.4	-9.78	-9.55	-10.13	-9.21	-9.76
	Longitude (deg)	-56.0	-40.4	-26.45	-11.8	1.47	15.4	30.47	43.64	57.6
	Right/left sense of c. p.	L	L	L	R/L	R/L	R/L	R/L	R/L	R/L
	QTR height (R_{\odot})*	0.084	-	-	-	-	-	-	-	-
NOAA 9415 April 9, 2001	Latitude (deg)		-21.6	-21.7	-21.3	-21.1	-20.0	-20.7	-20.9	-20.3
	Longitude (deg)		-42.5	-28.9	-15.9	-4.1	12.6	23.9	38.7	51.3
	Right/left sense of c. p.		L	L	-	R/L	-	-	R	R
	QTR height (R_{\odot})*		0.097	0.081	-	-	-	0.086	0.111	-

*The coronal heights in the QTR are calculated according to the procedure presented in Appendix B, for which purpose the displacements of the point $P = -0.1$ at the latitude of peak brightness in total intensity for the corresponding microwave source are measured.

APPENDIX 8: HEIGHT EVALUATION PROCEDURE

Let us indicate with Q a point in the QTR (see Fig 10) where the circular polarization at a given wavelength is transformed into zero circular polarization according to Eqs. (1) and (2), and with P its projection on the microwave source along the line of sight. In our treatment we will assume that the height h of Q ($h=QN$ in Fig. 10) is constant during the longitudinal displacement $\Delta\theta$ due to solar rotation and that the QTR is vertical. The point N is vertical projection of Q.

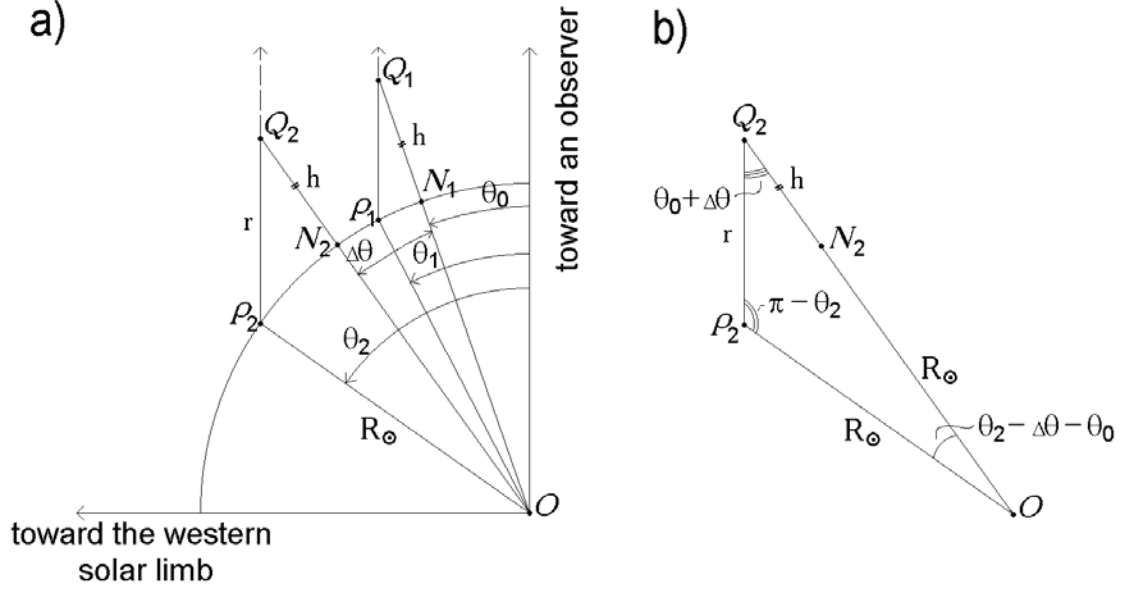


Fig. 10. Illustrative sketch showing the displacement due to solar rotation, from position 1 to 2, of the following points: one located on the microwaves source (P), one, Q, located in the QTR, where the circularly polarized radiation coming from P is cancelled, and one, N, is vertical projection of Q on the photosphere. The points are marked on the western quadrant of the Sun (a). Panel (b) shows the relations between the angles in the heliocentric triangle Q_2OP_2 , where $\Delta\theta$ is the longitudinal displacement due to solar rotation.

Applying the sinus theorem to the triangles Q_1OP_1 and Q_2OP_2 , we get

$$h = R_o \left(\frac{\sin \theta_1}{\sin \theta_0} - 1 \right) \quad (5)$$

for the height h and

$$\text{ctg } \theta_0 = \frac{\sin \theta_2 - \cos \Delta\theta \sin \theta_1}{\sin \theta_1 \sin \Delta\theta}. \quad (6)$$

for the unknown angle θ_0 .

The results of the coronal height calculations (Table I) are derived using the points of the $P = -0.1$ line, as more distinguishable than the $P = 0$ line in the microwave sources under consideration. According to Eq. (4), the normalized polarization $P = -0.1$ corresponds to the magnetic field $B = 21$ G measured at the wavelength 5.2 cm in the QT-region.